Carbohydrate Polymers 110 (2014) 456–463

Contents lists available at ScienceDirect

Carbohydrate Polymers

journal homepage: www.elsevier.com/locate/carbpol

A novel green approach for the preparation of cellulose nanowhiskers from white coir

Diego M. Nascimento[a], Jessica S. Almeida[b], Amanda F. Dias[c], Maria Clea B. Figueirêdo[d], João Paulo S. Morais[e], Judith P.A. Feitosa[a], Morsyleide de F. Rosa[d,*]

[a] Universidade Federal do Ceará (UFC), Centro de Ciências, Campus do Pici, Departamento de Química Orgânica e Inorgânica, Bloco 940, CEP 60455-760 Fortaleza, Ceará, Brazil
[b] Universidade Estadual do Ceará (UECE), Centro de Ciências, Campus do Itapery, Bloco S, CEP 60455-900 Fortaleza, Ceará, Brazil
[c] Instituto Federal de Educação, Ciência e Tecnologia do Ceará (IFCE), Campus Maracanaú, Departamento de Química e Meio Ambiente, CEP: 61939-140, Maracanaú, Ceará, Brazil
[d] Embrapa Agroindústria Tropical – CNPAT, Rua Dra Sara Mesquita 2270, Planalto do Pici, CEP 60511-110, Fortaleza, Ceará, Brazil
[e] Embrapa Algodão – CNPA, Rua Oswaldo Cruz 1143, Centenário, CEP 58428-095, Campina Grande, Paraíba, Brazil

ARTICLE INFO

Article history:
Received 9 February 2014
Received in revised form 4 April 2014
Accepted 17 April 2014
Available online 24 April 2014

Keywords:
Agribusiness
Nanotechnology
Green chemistry
Cellulose nanocrystal

ABSTRACT

The aim of this work was to optimize the extraction of cellulose nanowhiskers (CNW) from unripe coconut husk fibers (CHF). The CHF was delignified using organosolv process, followed by alkaline bleaching (5% (w/w) H_2O_2 + 4% (w/w) NaOH; 50 °C, 90 min). The CHF was subsequently hydrolyzed with 30% (v/v) sulfuric acid (60 °C, 360 min). The process yielded a partially delignified acetosolv cellulose pulp and acetic black liquor, from which the lignin was recovered. The CNW from the acetosolv pulp exhibited an average length of 172 ± 88 nm and a diameter of 8 ± 3 nm, (aspect ratio of 22 ± 8). The surface charge of the CNW was −33 mV, indicating a stable aqueous colloidal suspension. The nanocrystals presented physical characteristics close to those extracted from cellulose pulp made by CHF chlorine-pulping. This approach offers the additional advantage of extracting the lignin as an alternative to eradication.
© 2014 Elsevier Ltd. All rights reserved.

1. Introduction

Cellulose nanowhiskers (CNW), sometimes referred to as whiskers, are structures in nanoscale dimensions with a wide range of applications in different fields. Key applications of these structures involve their use as support systems for synthesis of metallic nanoparticles (Xiong, Lu, Zhang, Zhou, & Zhang, 2013), intelligent or active packages (Azeredo, Miranda, Rosa, Nascimento, & De Moura, 2012), and engineered nanocomposites (Eichhorn et al., 2010). CNW can replace carbon nanotubes as fillers because of their relatively low cost of production, easy obtainment process, low density (about 1.566 g/cm^3), non-abrasive nature, biocompatibility, and biodegradability (Postek et al., 2011).

Several sources of CNW like wood, non-wood fibers, algae, tunicates, and bacterial cellulose have been reported (Eichhorn et al., 2010). However, unripe coconut husk fiber (CHF) represents an exceptional major source of cellulose for the extraction of the CNW because it is significantly abundant, low-cost, and is an underutilized byproduct produced in several tropical regions (Rosa et al., 2010).

It has already been reported that CNW from CHF possess diameters smaller than 5 nm and an aspect ratio of 39 ± 14 (Rosa et al., 2010). In the work of Rosa et al. (2010), CHF were subjected to a series of treatments involving: (i) washing with hot water, (ii) bleaching with sodium chlorite ($NaClO_2$), (iii) pre-hydrolysis with nitric acid (HNO_3), and (iv) acidic hydrolysis with sulfuric acid (H_2SO_4, 64% (w/w)). Although it was possible to obtain a stable colloidal suspension, it presented a dark-brown aspect, which limited its use as filler in nanocomposites for films and packages, mainly owing to the presence of residual lignin (Rosa et al., 2010). Another limitation of this approach in pulping was the use of the chloro-based compound, $NaClO_2$, which is known to be detrimental to the

* Corresponding author at: Embrapa Agroindústria Tropical – CNPAT, Rua Dra. Sara Mesquita 2270, Planalto do Pici, CEP 60511-110, Fortaleza, Ceará, Brazil. Tel.: +55 85 3391 7344; fax: +55 85 3391 7109.
E-mail addresses: diego@alu.ufc.br (D.M. Nascimento), jeh.quimica@gmail.com (J.S. Almeida), joao.morais@embrapa.br (J.P.S. Morais), judith@dqoi.ufc.br (J.P.A. Feitosa), morsyleide.rosa@embrapa.br, morsyleide@gmail.com (M.F. Rosa).

http://dx.doi.org/10.1016/j.carbpol.2014.04.053
0144-8617/© 2014 Elsevier Ltd. All rights reserved.

environment owing to its role in the formation of organochlorine byproducts.

Usually, the higher the lignin content in a fiber, the higher the amount of reagents required to remove it and allow access to cellulose in order to produce CNW. However, lignin can be extracted as a separate product from CHF, using approaches that are closer to green chemistry and biorefinery principles (Ng, Tay, & Ng, 2013).

The aim of this work was to optimize the experimental conditions for the extraction of CNW from CHF, with a view to extracting cellulose and lignin through a chlorine-free pulping approach that allows for minimizing the waste of lignin, while using easily recoverable and low-environmental impact reagents. The physical and chemical properties of CNW were evaluated by analysis of surface charge, crystallinity index, crystal size dimension, FTIR spectroscopy, and thermogravimetric analysis. These results were compared to the already existing methods to produce CNW from CHF.

2. Methods

2.1. Material

Unripe coconut husk fiber (CHF) was collected as a city waste in Fortaleza, Ceará State, Brazil, and processed in a pilot plant processing unit from where it was transported to Embrapa Tropical Agroindustry (CNPAT), also in Fortaleza. The raw CHF was ground in Wilye mill (FORTINOX – STAR FT 80) with a 1.0 mm sieve. All solvents and reagents were of analytical grade and were used as received without any modification. The reagents 97% (w/w) NaOH, 37% (w/w) HCl, 30% (w/w) H_2O_2, 99.7% (w/w) acetic acid (AcOH), and 98% (w/w) H_2SO_4 were obtained from Vetec Química Fina Ltda – Duque de Caxias, RJ, Brazil, while 80% (w/w) $NaClO_2$ was obtained from Sigma–Aldrich, Saint Louis, MO, USA.

2.2. Acetosolv pulping (AP)

The CHF fibers were cooked in a mixture of 93% (w/w) AcOH and 0.3% (w/w) HCl in a hydrothermal reactor at 110 °C, in a ratio of 1:10 (w/v fiber:solution) with constant stirring for 180 min. At the end of the reaction, the mixture was separated into solid (acetosolv pulp) and liquid fractions (black liquor). The acetosolv pulp (AP) was washed with fresh AcOH (80 °C) to prevent lignin redeposition on the fiber. The black liquor (BL) was stored for further separation of the recovered lignin (RL) (Benar & Schuchardt, 1994).

2.3. Generation of recovered lignin (RL)

The BL was concentrated in a rotary evaporator (BUCHI – R-210/215) to recover the acetic acid. After this step, the volume of BL was diluted 10 times with distilled water at 80 °C to precipitate the lignin. The RL was filtered and washed with distilled water at 25 °C until it reached a pH close to the washing water. Subsequently, it was dried in a vacuum desiccator with silica gel.

2.4. Alkaline-peroxide bleaching (APB)

The AP was bleached with a solution of 5% (w/w) H_2O_2 and 4% (w/v) NaOH in a beaker at 50 °C in a ratio of 1:20 (fiber:solution, w/v) with constant stirring for 90 min. At the end of the reaction, the bleached acetosolv pulp (BAP) was vacuum-filtered and washed with distilled water until it reached the pH of water used in the washing step. The BAP was oven-dried at 50 °C for 24 h, and then the bleaching procedure was repeated.

2.5. Extraction of cellulose nanowhiskers (CNW)

The final BAP was stirred in a 30% (v/v) (43.6%, w/w or 8 mol/L) solution of H_2SO_4 at 60 °C, in a 1:8.75 (w/v) ratio of fiber:solution for 360 min (Wang, Cao, & Zhang, 2006). At the end of the process, the reaction was halted by adding 10 times the volume of cold deionized water (~10 °C). The colloidal suspension was centrifuged in three cycles of 13,000 rpm (26,400 × g) (HITACHI – CR 22GIII) for 15 min until the supernatant began to turn turbid. In other words, in the first and in the second centrifugations, the supernatant was clear, and the CNW were in the bottom; in the third centrifugation, the supernatant began to become turbid, indicating that the CNW were beginning to leak to the supernatant. Between each centrifugation, the suspension was ultra-sonicated (UNIQUE – Cell Disruptor – 500 W) at 90% power for 5 min to prevent the formation of agglomerates. Thereafter, the suspension was dialyzed with tap water for 24 h until it reached a pH of 6–7. The suspension was ultra-sonicated at the end of the dialyses as described previously, prior to characterization.

2.6. Characterization

2.6.1. Chemical characterization of fibers

The CHF, AP, and BAP fibers were chemically analyzed. The moisture, extractive, and Klason lignin contents were determined in accordance to TAPPI T 421 om-02 (2002), TAPPI T 204 cm-97 (1997), and TAPPI T 222 om-22 respectively (2000). Hemicellulose and alpha-cellulose contents were analyzed as described by Yokoyama, Kadla, and Chang (2002) and TAPPI T 203cm-99 (2009). The results are presented in dry weight of fibers.

2.6.2. FTIR analysis

Samples of CHF, AP, BAP, and RL were ground and pelletized using KBr (1:50, w/w). The spectra were recorded in the range of 4000 cm^{-1} to 400 cm^{-1} (Agilent Cary 640 FTIR) using Fourier transformation.

2.6.3. Electron microscopy

The three different fibers (CHF, AP, and BAP) were analyzed by scanning electronic microscopy (SEM). All fibers were metalized (Emitech K550) with gold sputtering prior to examination and scanned at an acceleration voltage of 15 kV (Zeiss DSM 940A).

The CNW were measured by transmission electronic microscopy (TEM). A volume of 1 mL of nanocellulose 5% (w/v) suspension was dropped onto a Formvar™/Carbon support with a 300 mesh copper grid. After 2 min, the excessive water was drained with a Whatmann paper no.2, and the grid was inverted and allowed to touch a drop of 2% (w/v) uranyl acetate for 5 min. This process was repeated three times, and the grid was air-dried at room temperature for 24 h. The grids were examined in a JEOL JEM 1200FxII microscope. The length and width of 100 crystals were recorded using the software GNU Image Manipulation Program (GIMP 2.8).

2.6.4. X-ray diffractogram

Samples of CHF, AP, BAP, and dried CNW were analyzed in an Xpert MPD diffractometer with Co tube in 40 kV and 40 mA in the 2θ range from 3° to 50°. The crystallinity index (CI) was calculated as the ratio between the integrated area of all crystalline peaks and the integrated total area (Rabek, 1980). The diffractogram peak deconvolution was performed with the Gausian function of the software PeakFit® of Systat Software Inc (SigmaPlot™), using the following equation:

$$\mathrm{CI}\,(\%) = \frac{I_C}{I_C + I_A} \quad (1)$$

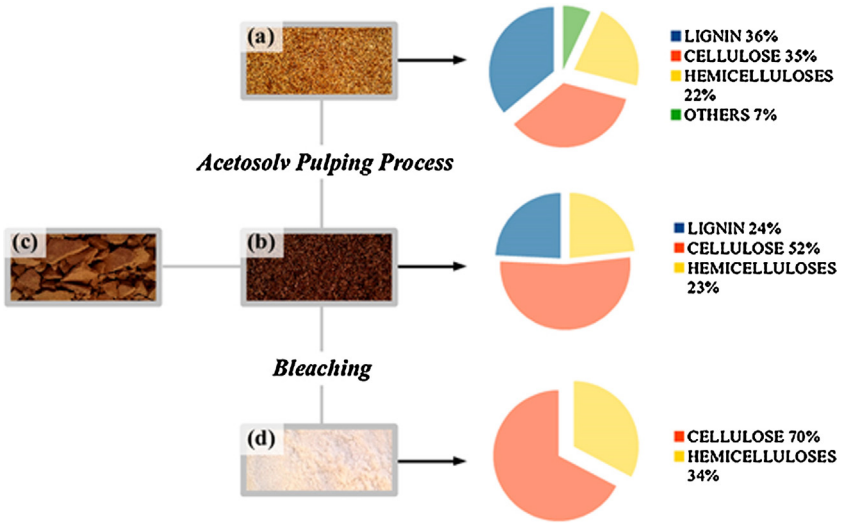

Fig. 1. Chemical composition (dry basis) of (a) unripe coconut husk fiber (CHF), (b) acetosolv pulp (AP), (c) recovered lignin (RL), and (d) bleached acetosolv pulp (BAP).

in which CI (%) is the percentage crystalline fraction, I_C is the total area of crystalline peaks and I_A is the total area of the amorphous region.

The size of the perpendicular crystal to the plane 0 0 2 (τ) was estimated using the Scherrer's equation (Patterson, 1939):

$$\tau = \frac{0.9\lambda}{\beta_{002} \times \cos\theta_{002}} \quad (2)$$

where β_{002} is the line broadening at half the maximum intensity (FWMH) of diffraction plane 0 0 2; θ_{002} is the maximum diffraction angle of plane 0 0 2, and λ is the wavelength of the X-ray source (0.178 nm).

2.6.5. Thermal analyses

The CHF, AP, BAP, and dried CNW were analyzed in a Mettler Toledo TGA/SDTA 851 under a N_2 atmosphere with a 50 mL/min gas flow rate, heating rate of 10 °C/min, and a temperature range from 25 to 800 °C, in an alumina sample holder.

2.6.6. Zeta potential and particle size measurement

A sample of 1 mL of the suspension of CNW was diluted to a ratio of 1:50 (v/v) and three replicates of 0.75 mL were analyzed in folded capillary cell (DTS1060) in a Malvern 3000 Zetasizer NanoZS to determine the surface charge and estimate the crystal size using diffraction light scattering (DLS). The particle size was measured using the Smoluchowski algorithm (Lang & Xanh, 1980; Tournier, Fitzjohn, & Bates, 2006).

3. Results and discussion

3.1. Chemical characterization, CNW extraction, and recovery of lignin

After the bleaching and acetosolv pulping steps, the content of non-cellulosic components decreased significantly (Fig. 1).

The CHF presented 35% of α-cellulose and 36% of Klason lignin contents, which are similar to the values obtained by Muensn, Kunanopparat, Menut, and Siriwattanayotin (2011). This team studied the chemical properties of several coconut varieties and found cellulose contents around ~33% and ~42% lignin contents. In our case, the acetosolv pulping increased the cellulose content, eliminated some of the extractives and non-cellulose carbohydrates, while reducing the lignin content in the fiber from 36% to 24%. Furthermore, the bleaching treatment efficiently eliminated the residual lignin, which increased the accessibility of cellulose to promote acidic hydrolysis, resulting in a light-cream nanocellulose suspension (Section 3.3).

Acetosolv pulping removed much of the CHF lignin and some hemicellulose as reported in other works (Li, Sun, Xu, & Sun, 2012). Moreover, it appeared to weaken the residual lignin in the fibers. Previous work by Rosa et al. (2010) had reported four serial chlorine bleaching procedure to successfully eliminate the bulk of the CHF lignin. Despite the additional acid hydrolysis of the cellulose pulp, the obtained suspension was still dark-brown in color, indicating the presence of residual lignin.

The mass balance of the process (Fig. 2) implied a fair efficient removal of lignin from the fiber. In addition, limited amounts of polysaccharides were removed in the black liquor, with a recovery yield of ~50% of lignin from the CHF. Up to 24% of the total lignin in the raw CHF was extracted, and the recovered lignin represented 18% of the 36% starting material (Fig. 2). The lignin recovery yield in the black liquor is in agreement with acetosolv extractions in softwood, hardwood and non-woody biomasses (Soudham, Rodriguez, Rocha, Taherzadeh, & Martin, 2011). Therefore, it seems plausible that the lignin recovery as a pulping byproduct in this approach might contribute to increase the economic viability of the whole process, however further in depth analyses are crucial to confirm these findings (Figueirêdo et al., 2012; Rosa et al., 2010).

After the treatments, it was possible to obtain a yield of up to 50% of AP, 22% of BAP, and 12% of CNW. The yield of CNW represented 54.5% of BAP content. Meanwhile, traditional chlorine-based pulping (Figueirêdo et al., 2012; Rosa et al., 2010) yielded values of 23% for BAP, and only 6% for CNW, whereas the lignin could not be recovered. This suggests that acetosolv pulping was efficient in increasing the CNW yield and produced a second byproduct with economic value, which, in other processes, is commonly regarded as a waste.

3.2. FTIR analysis

The FTIR graphics corroborate the chemical characterization of the fibers (Section 3.1) and the effect of the chemical treatments (Fig. 3, Table 1) in addition the efficiency of lignin recovery is also confirmed.

All the spectra of fibers displayed bands at 3400 cm^{-1} due to the hydroxyl groups, at 2925 cm^{-1} due to —CH stretching, at 1640 cm^{-1} as a result of water angular deformation, and at 896 cm^{-1} due to polysaccharide glycoside bonds (Silverstein, Bassler, & Morrill, 1991; Socrates, 2004).

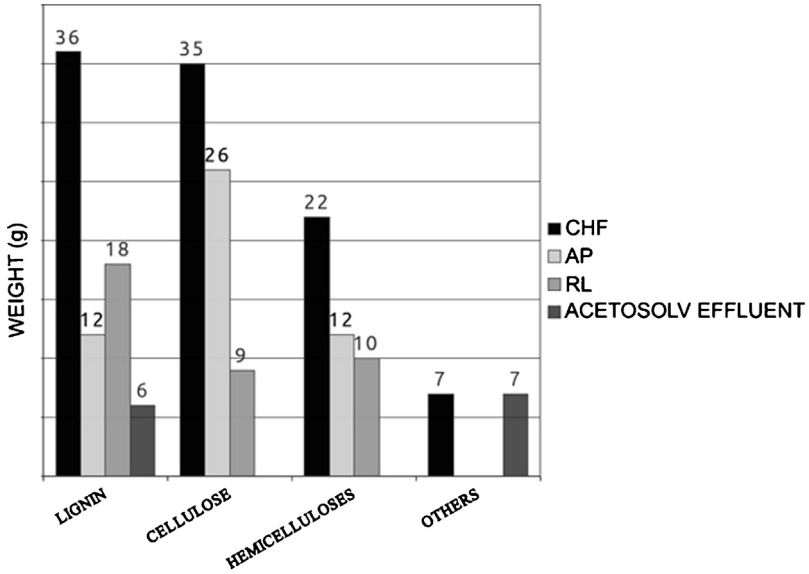

Fig. 2. Mass balance of the acetosolv step with the lignocellulosic component contents in 100 g of unripe coconut husk fiber (CHF), acetosolv pulp (AP), in recovered lignin (RL), and in the acetosolv effluent.

The band at 1730 cm^{-1} in the CHF and AP is related to C=O stretching from ketone and/or esters of hemicellulose, or carboxyl groups of lignin (Sun, Xu, Sun, Fowler, & Baird, 2005). The presence of lignin is depicted by the band at 1500 cm^{-1}, which represents the stretching of aromatic ring and the band at 1079 cm^{-1}, which represents the C=C bond of the aromatic ring (Sun et al., 2005). As the fiber was subjected to chemical pulping and bleaching, the intensities of all of these peaks were reduced, indicating the partial removal of lignin and hemicellulose.

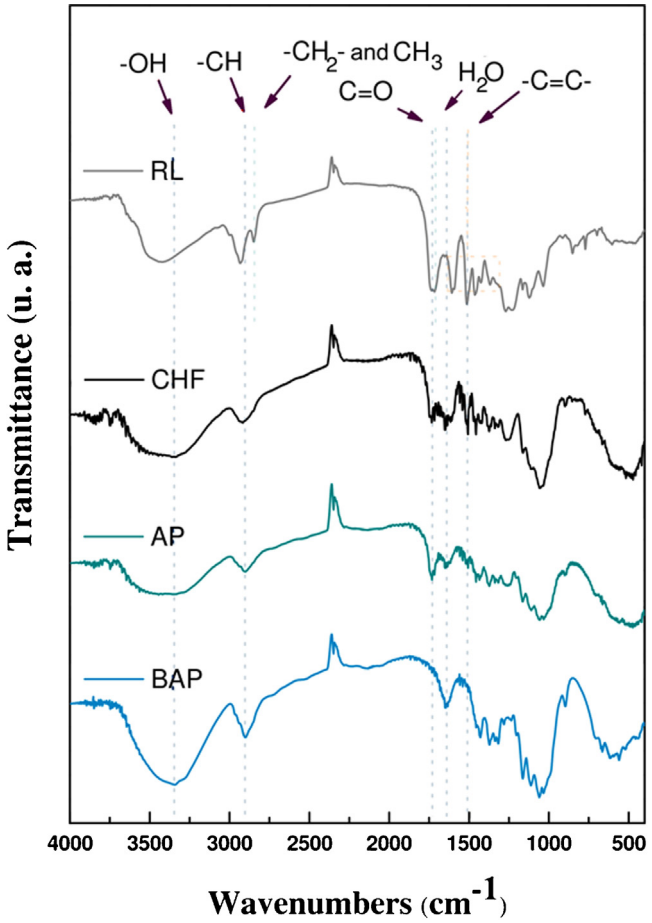

Fig. 3. FTIR spectra for: recovered lignin (RL), unripe coconut husk fiber (CHF), acetosolv pulp (AP), and bleached acetosolv pulp (BAP).

The spectrum of RL presents phenolic and aliphatic hydroxyl groups (3400 cm^{-1} and 1370 cm^{-1}), —CH stretching of —O—CH_3 aromatic ethers (2900 cm^{-1}), —CH_3 and —CH_2 side chains (2810 cm^{-1}), —C=O stretching (1730 cm^{-1}), and C=C aromatic structural vibrations (1604 cm^{-1}, 1500 cm^{-1}, and 1450 cm^{-1}). Moreover, it was possible to note weak peaks related to C_1—H bonds of the anomeric carbon in β (850 cm^{-1}) and α (930 cm^{-1}) configurations, indicating residual carbohydrates from the hemicellulose hydrolysis (Li et al., 2012).

3.3. Electron microscopy

The chemical processing of the CHF to BAP clearly affected the surface of the fibers (Fig. 4). The CHF presents a compact and flat surface, while AP and BAP fibers are loose and rough. The pulping and bleaching treatments removed part of the macromolecules (Section 3.1), affecting the overall fiber surface (Johar, Ahmad, & Dufresne, 2012). Bleaching induced the formation of pits on the fiber, which is known to increase the surface area and ease the acidic hydrolysis of the carbohydrates.

The CNW produced after acid treatment was analyzed using TEM (Fig. 5) to evaluate the aspect ratio of the crystals. The whiskers were in the form of long and disordered needles with a

Table 1
Vibrational frequencies (cm^{-1}) in the FTIR spectra of the unripe coconut husk fiber (CHF), acetosolv pulp (AP), bleached acetosolv pulp (BAP), and recovered lignin.

Wavenumber (cm^{-1})	Peak assignment
~3400	(OH) str.
~2900	(CH_2 and CH_3) str.
~1730	(C=O) str. in conjugated acids or esters with aromatic rings
~1640	(OH) def. due to adsorved H_2O
~1500	(C=C) vibr. of aromatic ring in lignin
~1255	(C_5—O—C_1) str. in hemicellulose
~896	(C_1—O—C_4) str. in cellulose

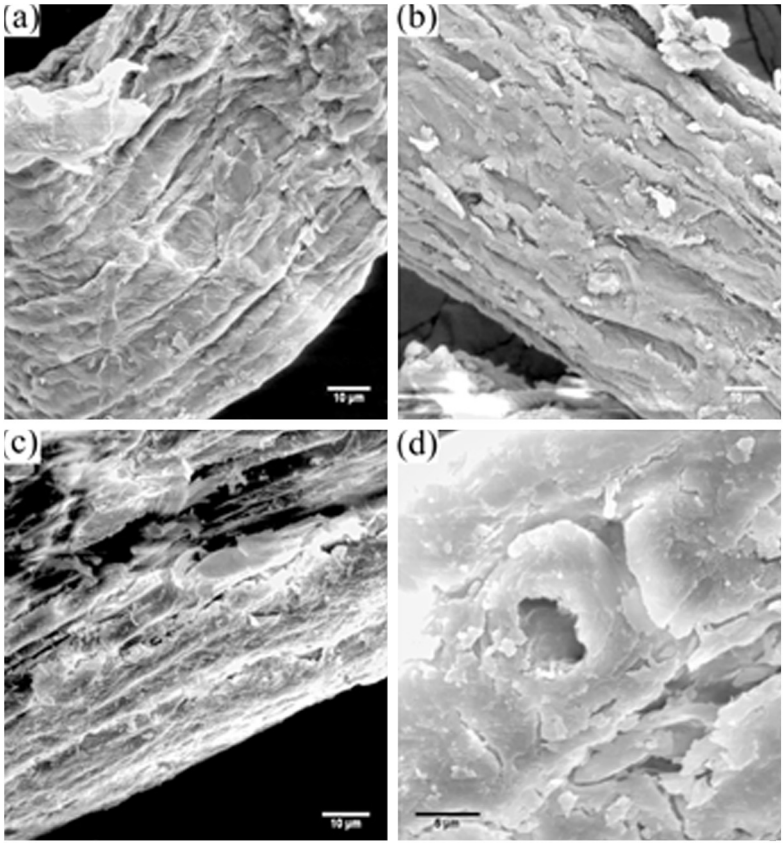

Fig. 4. SEM picture of (a) unripe coconut husk fiber (CHF), (b) acetosolv pulp (AP), and (c–d) bleached acetosolv pulp (BAP).

bundle-formation trend, resulting from the interatomic forces such as hydrogen bonding (Elazzouzi-Hafraoui et al., 2008).

On average, the CNW were 172 ± 88 nm in length and 8 ± 3 nm in width, yielding an aspect ratio of 22 ± 8. Rosa et al. (2010) obtained CNW with an aspect ratio of 39 ± 14, but the process was notably different from the acetosolv pulping approach.

Aspect ratio is a function of the lignocellulosic source. Depending on the source, the values of the aspect ratio are variable. For instance, a ratio of 8–10 is observed for cotton white lint (Teixeira et al., 2010), 15–20 for rice husk (Johar et al., 2012), and 19 for cotton linter (Morais et al., 2013).

The aspect ratio of CNW directly reflects their ability to distribute mechanical stress in the interface matrix/filler. The higher the aspect ratio of the nanocrystal, the greater the reinforcement and mechanical barrier properties in the nanocomposite to which they are applied (Johar et al., 2012). So, although the aspect ratio of CNW from the BAP is lower than that of CNW from a chlorine-pulped fiber (Rosa et al., 2010), the values obtained for acetosolv-pulped nanocrystals are within the typical range for other fillers in nanocomposites.

3.4. Zeta potential and DLS measurement

The CNW in this work presented a zeta potential of around −33 mV, on this basis, it was considered to be a stable suspension (Zhou, Fu, Zheng, & Zhan, 2012). However, the zeta potential could not be compared directly with other CHF nanowhiskers (Fahma, Iwamoto, Hori, Iwata, & Takemura, 2011; Rosa et al., 2010). Nevertheless, the nanostructures exhibited a surface charge similar to what has been observed previously for cotton white lint (−31 mV) (Teixeira et al., 2010).

These results are in accordance with the observation by TEM (Section 3.3), because the crystals are water-stable due to sulfate groups, whose negative surface charge repels the nanoparticles in a stable system (Zhou et al., 2012).

The DLS measurements are related to the Brownian motion of the nanoparticles, in which small particles can move faster than large counterparts (Braun, Dorgan, & Chandler, 2008). The CNWs from the BAP presented two main peaks, at 44 nm (42% of counts) and 180 nm (58%). The peak at 180 nm corroborates the observed length of crystals by TEM, which was ~172 nm (Section 3.3). The differences in TEM and DLS measurements may potentially be a result of the DLS technique, which measures the hydrodynamic radius in colloid suspensions and is more biased to large sized particles than small sized (Oliveri, Elliott, Carnes, Hutchison, & Johnson, 2013).

3.5. X-ray diffraction

The crystallinity index of cellulose in the fibers was notably affected by chemical treatments (Table 2) and all the samples presented diffraction patterns typical of cellulose I, as expected for cobalt radiation (Bonarski & Olek, 2011), with peaks at 17° (plane

Table 2
Crystallinity indexes and crystallite average size in the plane 0 0 2 as determinated by XRD for unripe coconut husk fiber (CHF), acetosolv pulp (AP), bleached acetosolv pulp (BAP), and cellulose nanowhisker (CNW).

Sample	Crystallinity index (%)	Crystallite size (D_{002}) (nm)
CHF	54	3.1
AP	72	3.8
BAP	79	4.6
CNW	82	5.0

Fig. 5. TEM pictures for cellulose nanocrystals from the bleached acetosolv pulp (BAP), and a picture of a sample of the nanocrystal suspension.

1 0 1), 19° (plane 1 0 $\bar{1}$), 26° (plane 0 0 2), and 41° (plane 0 4 0). Thus, the crystallinity index of the samples changed, but the structure of the crystal was not affected by these chemical modifications. The extractions of the CNW was carried out with a low concentration of sulfuric acid (43.6%, w/w) in comparison to the most commonly reported recipe (64%, w/w) (Habibi, 2014). Therefore, some amount of amorphous cellulose may be present in the CNW.

The dimensions of the crystals related to plane 0 0 2 and crystallinity index increased as the chemical treatments were performed, probably due to recrystallization of the amorphous regions in the border of the crystalline regions in the cellulose fiber. As the hydroxyl groups from cellulose can form new hydrogen bonds between them in the amorphous components as a result of hemicellulose and lignin removal (Sections 3.1–3.3) (Eichhorn et al., 2010).

After the acid hydrolysis of BAP, the crystallinity of cellulose increased. However, due to the surface phenomena, the crystallinity index never reaches 100%, because the glucose molecule at the end of cellulose fibril cannot form hydrogen bonds with an additional cellulose molecule in the adjacent fibril (Eichhorn et al., 2010).

The crystallinity index of these nanocrystals (82%) is higher than the index of chlorine-pulped fibers from Fahma et al. (2011), which reached 57%, and the index of Rosa et al. (2010), which reached 66%. Hence, the acetosolv-pulped nanocrystals from CHF are potentially more suitable as fillers for nanocomposites than chlorine-pulped nanocrystals from CHF.

3.6. Thermal analysis

All the materials presented initial weight loss around 100 °C, mainly due to water loss (Fig. 6). The graph of CHF presents a similar tendency when compared to the graph from Rosa et al. (2010). The CHF presented two events of weight loss (Fig. 6); one with onset at 260 °C, having 23% of weight loss and the presence of a peak at 288 °C, and the second with onset at 330 °C, having 52% weight loss and a peak at 343 °C. The former event is related to thermal depolimerization of hemicelluloses, while the latter is due to cellulose degradation (Morán, Alvarez, Cyras, & Vázquez, 2008). As lignin is more thermally stable than carbohydrates, it presents a broader decomposition range, overlapping with other lignocellulosic components (D'almeida, Barreto, Calado, & D'almeida, 2008).

AP and BAP showed a single main event. The AP onset was at 337 °C, with 73% weight loss, with a peak observed at 359 °C, while the BAP onset was at 330 °C, with 87% weight loss and a peak at 351 °C. The removal of hemicellulose and lignin (Sections 3.1 and 3.4) increased the cellulose content in the two different fibers, accentuating the dTG peaks and improving the thermal stability in comparison to the CHF. The higher residue at 800 °C in AP can be related to the higher lignin content than in BAP fiber. Lignin is more likely to produce char than cellulose, because of the condensation of aromatic rings in an inert atmosphere (Morán et al., 2008).

The CNW also presented a single main weight loss, with onset at 270 °C, loss of 77% of the weight, and a peak at 311 °C. The

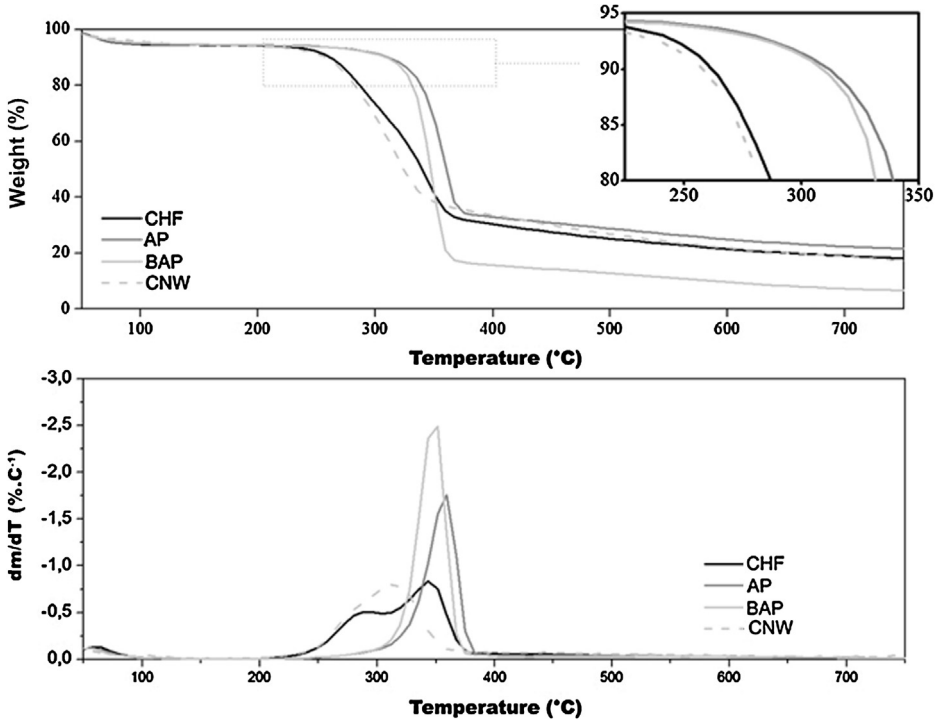

Fig. 6. TGA and dTG of the: (a) unripe coconut husk fiber (CHF), (b) acetosolv pulp (AP), (c) bleached acetosolv pulp (BAP), and (d) cellulose nanowhisker (CNW).

reduction in thermal stability in comparison to AP and BAP is due to the insertion of sulfate groups (Section 3.3), which catalyze the thermal degradation of the carbohydrate structure (Zhou et al., 2012).

4. Conclusions

The organosolv pulping was efficient in separating lignin from coconut husk fibers. The organosolv-pulped fiber was bleached to a carbohydrate material from which it was possible to extract cellulose nanowhiskers with characteristics similar to nanocrystals from chlorine-pulped fibers.

This organosolv pulping method is more suitable as a biorefinery approach than a chlorine-pulping approach because the lignocellulosic biomass resulting from it is better separated, with less waste of lignin. Moreover, the use of a low concentration of sulfuric acid (43.6%, w/w versus 64%, w/w) to extract the cellulose nanowhiskers can also be an important greener chemistry approach. Further critical studies must be conducted in order to optimize the utilization of extractives and hydrolyzed hemicellulose and to analyze the environmental impact this approach may have through by life cycle analyses.

Acknowledgements

This work was funded by Embrapa and CNPq. The authors thank the Laboratório de Raios X at Universidade Federal do Ceará for the X-rays analyses, the Laboratório de Produtos e Processos at Universidade Federal do Ceará for the thermal analyses, and the Universidade Federal de São Carlos for the TEM analyses.

References

Azeredo, H. M. C., Miranda, K. W. E., Rosa, M. F., Nascimento, D. M., & De Moura, M. R. (2012). Edible films from alginate-acerola puree reinforced with cellulose whiskers. *Food Science and Technology*, *46*, 294–297.

Benar, P., & Schuchardt, U. (1994). Eucalyptus Acetosolv pulping–optimization of the cooking conditions and characterization of the pulp and lignin. *Cellulose Chemistry and Technology*, *28*, 435–444.

Bonarski, J. T., & Olek, W. (2011). Application of the crystalline volume fraction for characterizing the ultrastructural organization of wood. *Cellulose*, *18*, 223–235.

Braun, B., Dorgan, J. R., & Chandler, J. P. (2008). Cellulosic nanowhiskers. Theory and application of light scattering from polydisperse spheroids in the Rayleigh–Gans–Debye regime. *Biomacromolecules*, *9*, 1255–1263.

D'almeida, A. L. F. S., Barreto, D. W., Calado, V., & D'almeida, J. R. M. (2008). Thermal analysis of less common lignocellulose fibers. *Journal of Thermal Analysis and Calorimetry*, *91*, 405–408.

Eichhorn, S. J., Dufresne, A., Aranguren, M., Marcovich, N. E., Capadona, J. R., Rowan, S. J., et al. (2010). Review: Current international research into cellulose nanofibres and nanocomposites. *Journal of Materials Science*, *45*, 1–33.

Elazzouzi-Hafraoui, S., Nishiyama, Y., Putaux, J., Heux, L., Dubreuil, F., & Rochas, C. (2008). The shape and size distribution of crystalline nanoparticles prepared by acid hydrolysis of native cellulose. *Biomacromolecules*, *9*, 57–65.

Fahma, F., Iwamoto, S., Hori, N., Iwata, T., & Takemura, A. (2011). Effect of pre-acid-hydrolysis treatment on morphology and properties of cellulose nanowhiskers from coconut husk. *Cellulose*, *18*, 443–450.

Figueirêdo, M. C. B., Rosa, M. F., Ugaya, C. M. L., Souza Filho, M. S. M., Silva Braid, A. C. C., & Melo, L. F. L. (2012). Life cycle assessment of cellulose nanowhiskers. *Journal of Cleaner Production*, *35*, 130–139.

Habibi, Y. (2014). Key advances in the chemical modification of nanocelluloses. *Chemical Society Reviews*, *43*, 1519–1542.

Johar, N., Ahmad, I., & Dufresne, A. (2012). Extraction, preparation and characterization of cellulose fibres and nanocrystals from rice husk. *Industrial Crops and Products*, *37*, 93–99.

Lang, R., & Xanh, N. X. (1980). Smoluchowski's theory of coagulation of colloids holds rigorously in the Boltzmann-Grad limit. *Zeitschrift für Wahrscheinlichkeitstheorie und Verwandte Gebiete*, *54*, 227–280.

Li, M.-F., Sun, S.-N., Xu, F., & Sun, R.-C. (2012). Mild acetosolv process to fractionate bamboo for the biorefinery: Structural and antioxidant properties of the dissolved lignin. *Journal of Agricultural and Food Chemistry*, *60*, 1703–1712.

Morais, J. P. S., Rosa, M. F., Souza Filho, M. S. M., Nascimento, L. D., Nascimento, D. M., & Cassales, A. R. (2013). Extraction and characterization of nanocellulose structures from raw cotton linter. *Carbohydrate Polymers*, *91*, 229–235.

Morán, J. I., Alvarez, V. A., Cyras, V. P., & Vázquez, A. (2008). Extraction of cellulose and preparation of nanocellulose from sisal fibers. *Cellulose*, *15*, 149–159.

Muensn, P., Kunanopparat, T., Menut, P., & Siriwattanayotin, S. (2011). Effect of lignin removal on the properties of coconut coir fiber/wheat gluten biocomposite. *Composites Part A: Applied Science and Manufacturing*, *42*, 173–179.

Ng, R. T. L., Tray, D. H. S., & Ng, D. K. S. (2013). Simultaneous process synthesis, heat and power integration in a sustainable integrated biorefinery. *Energy & Fuels*, *26*, 7316–7330.

Oliveri, A. F., Elliott, E. W., III, CarnesF M.E., Hutchison, J. E., & Johnson, D. W. (2013). Elucidating inorganic nanoscale species in solution: Complementary and corroborative approaches. *ChemPhysChem*, *14*, 2655–2661.

Patterson, A. L. (1939). The Scherrer formula for X-ray particle size determination. *Physical Review*, *56*, 978–982.
Postek, M. T., Vladár, A., Dagata, J., Farkas, N., Ming, B., Wagner, R., et al. (2011). Development of the metrology and imaging of cellulose nanocrystals. *Measurement Science and Technology*, *22*, 1–10.
Rabek, J. F. (1980). *Experimental methods in polymer chemistry: Applications of wide-angle X-ray diffraction (WAXS) to the study of the structure of polymers*. Chichester: Wiley Interscience.
Rosa, M. F., Medeiros, E. S., Malmonge, J. A., Gregorski, K. S., Wood, D. F., Mattoso, L. H. C., et al. (2010). Cellulose nanowhiskers from coconut husk fibers: Effect of preparation conditions on their thermal and morphological behavior. *Carbohydrate Polymers*, *81*, 83–92.
Silverstein, R. M., Bassler, G. C., & Morrill, T. C. (1991). *Spectrometric identification of organic compounds* (5th ed.). New York: John Wiley & Sons.
Socrates, G. (2004). *Infrared and Raman characteristic group frequencies* (3rd ed.). New York: John Wiley & Sons.
Soudham, V. P., Rodriguez, D., Rocha, G. J. M., Taherzadeh, M. J., & Martin, C. (2011). Acetosolv delignification of marabou (*Dichrostachys cinerea*) wood with and without acid prehydrolysis. *Forestry Studies in China*, *13*, 64–70.
Sun, X. F., Xu, F., Sun, R. C., Fowler, P., & Baird, M. S. (2005). Characteristics of degraded cellulose obtained from steam-exploded wheat straw. *Carbohydrate Research*, *340*, 97–106.
TAPPI. (1997). *T 204 om-97. Solvent extractives of wood and pulp*.
TAPPI. (2000). *T 222 om-02. Acid-insoluble lignin in wood and pulp*.
TAPPI. (2002). *T 421 om-02. Moisture in pulp, paper and paperboard*.
TAPPI. (2009). *T 203 cm-99. Alpha-, beta- and gamma-cellulose in pulp*.
Teixeira, E. M., Corrêa, A. C., Manzoli, A., Leite, F. L., Oliveira, C. R., & Mattoso, L. H. C. (2010). Cellulose nanofibers white and naturally colored cotton fibers. *Cellulose*, *17*, 595–606.
Tournier, A. L., Fitzjohn, P. W., & Bates, P. A. (2006). Probability-based model of protein–protein interactions on biological timescales. *Algorithms for Molecular Biology*, *1*.
Wang, Y., Cao, X., & Zhang, L. (2006). Effects of cellulose whiskers on properties of soy protein thermoplastics. *Macromolecular Bioscience*, *6*, 524–531.
Xiong, R., Lu, C., Zhang, W., Zhou, Z., & Zhang, X. (2013). Facile synthesis of tunable silver nanostructures for antibacterial application using cellulose nanocrystals. *Carbohydrate Polymers*, *95*, 214–219.
Yokoyama, T., Kadla, J. F., & Chang, H.-M. (2002). Microanalytical method for the characterization of fiber components and morphology of woody plants. *Journal of Agriculture and Food Chemistry*, *50*, 1040–1044.
Zhou, Y. M., Fu, S. Y., Zheng, L. M., & Zhan, H. Y. (2012). Effect of nanocellulose isolation techniques on the formation of reinforced poly(vinyl alcohol) nanocomposite films. *Express Polymer Letters*, *6*, 794–804.